CARBON 50 (2012) 808–814

Available at www.sciencedirect.com

SciVerse ScienceDirect

journal homepage: www.elsevier.com/locate/carbon

New insights into the density of states of graphene oxide using capacitive photocurrent spectroscopy

Tanesh Bansal [a], Aditya D. Mohite [b], Hemant M. Shah [a], Charudatta Galande [c], Anchal Srivastava [c,1], Jacek B. Jasinski [d], Pulickel M. Ajayan [c], Bruce W. Alphenaar [a,*]

[a] Department of Electrical and Computer Engineering, University of Louisville, Louisville, KY, USA
[b] Los Alamos National Laboratory, NM, USA
[c] Department of Mechanical Engineering & Materials Science, Rice University, Houston, TX, USA
[d] Conn Center for Renewable Energy Research, University of Louisville, Louisville, KY, USA

ARTICLE INFO

Article history:
Received 16 May 2011
Accepted 18 September 2011
Available online 22 September 2011

ABSTRACT

Capacitive photocurrent spectroscopy is used to probe the electronic states of graphene-oxide, and reduced graphene-oxide. Three peaks are observed whose intensities scale with the oxygen coverage. The energy of these peaks correlate with the luminescence spectra reported for graphene-oxide. Using a fitting procedure, the density of states for graphene oxide is extracted from the data. It consists of the π/π^* states along with a distribution of mid-gap states centered at three different energies near the Dirac point. X-ray photoelectron spectroscopy measurements are used to identify the oxygen functional groups corresponding to the observed state distribution.

1. Introduction

Graphene is a semi-metal, with a continuous distribution of states available for the π-conduction electrons [1] and hence has relatively high conductivity. Graphene oxide (GO) on the other hand, is an insulator, with very low conductivity [2,3]. Theory suggests that the GO electronic density of states (DOS) varies non-monotonically with energy, and contains numerous gaps and peaks. The exact form of the DOS is predicted to depend on the oxygen coverage on the graphene surface [4,5]. For certain oxygen concentrations, semiconducting behavior is expected. This implies the possibility of tuning the GO conductivity by varying the oxygen concentration.

Optical spectroscopy is the primary experimental tool that has been used to explore the GO DOS. The GO absorbance spectrum is very broad with a peak at 5.4 eV, and a smaller shoulder at 3.9 eV. The main peak is thought to be due to the graphene π/π^* transition, while the shoulder has been attributed to the n–π^* transition of C=O. Photoluminescence spectra have been reported by three different groups. Luo et al. observe a broad photoluminescence peak centered at 1.65 eV which shifts to somewhat lower energy following reduction [6]. Nanometer scale strips of GO (measured by Sun et al.) show somewhat higher energy luminescence (2.18 eV) possibly because of quantum confinement [7]. Finally, measurements of reduced GO (rGO) by Eda et al. show much higher energy luminescence centered at 3.2 eV [8]. Thus, the GO optical spectrum clearly varies with the synthesis conditions and geometry; however, overall the measurements do not show an obvious decrease in band-gap with decreasing oxygen coverage.

Here we examine the DOS for GO and rGO using a new measurement technique called capacitive photocurrent spectroscopy, or CPS [9,10]. While similar to absorption spectroscopy, CPS is unique in that it specifically measures absorption due to the formation of charge carriers, while

* *Corresponding author:* Fax: +1 502 852 8128.
E-mail address: brucea@louisville.edu (B.W. Alphenaar).
[1] Present address: Department of Physics, Banaras Hindu University, Varanasi 221005, India.
0008-6223/$ - see front matter © 2011 Elsevier Ltd. All rights reserved.
doi:10.1016/j.carbon.2011.09.037

being uninfluenced by absorption due to vibrational states of the lattice, or non-mobile impurity states [11]. The capacitive photocurrent spectrum of GO has three dominant peaks. Two of these peaks match well with published optical spectroscopy data, while the third, low energy peak is new to the CPS measurement. A numerical fitting procedure is used to extract the GO DOS from the measured results. It is shown that the observed features can be ascribed to transitions between the π/π^* graphene levels and mid-gap states due to carboxyl groups. Reduction of the GO results in the re-emergence of the background density of states due to the graphene, along with additional states due to defects. The three peaks due to the GO also remain, indicating the continued presence of oxidized regions.

2. Experimental

GO was synthesized from graphite powder (SP-1 grade 325 mesh, Bay Carbon Inc.) by a modified Hummers method [12] as originally presented by Kovtyukhova et al. [13]. The graphite powder (12 g) is pre-oxidized in a solution of concentrated H_2SO_4 (50 ml), $K_2S_2O_8$ (10 g) and P_2O_5 (10 g). The mixture is then diluted with DI, filtered, washed and allowed to dry in air. For further oxidation, concentrated H_2SO_4 (460 ml) is added while maintaining the temperature at 0 °C using an ice bath. $KMnO_4$ (60 g) is added slowly while keeping the temperature under 10 °C and stirred for 2 h at 35 °C. After that, distilled water (920 ml) is added slowly while keeping the temperature under 50 °C. More DI water (2.8 l) and 50 ml of 30% H_2O_2 is added and allowed to settle for a day. The mixture is then centrifuged, washed with 10% HCl solution followed by DI water, dried in air and diluted further to make a 2% w/w dispersion that is put through dialysis for 2 weeks. Finally the GO sample is prepared by drop casting this 2% aqueous dispersion solution onto an ITO coated quartz substrate.

Reduced GO samples were synthesized by following the procedure presented by Wei Gao et al. [14]. Briefly, 1 g l^{-1} colloidal solution of dry GO in DI water is subjected to three step reduction process: de-oxygenation with $NaBH_4$ (Sodium borohydride) for 1 hr at 80 °C; dehydration with concentrated sulfuric acid at 120 °C with stirring for 12 h; and annealing at 1100 °C under a 1300 sccm gas flow of Ar/H_2 (15 vol%) for 15 min. The resulting solid is then dispersed in dimethylformamide (DMF) by sonication for 50 min. Finally, this dispersed solution is used to prepare the rGO samples by drop casting onto an ITO coated quartz substrate.

Capacitive photocurrent measurements were performed using the set-up shown in Fig. 1 [9,10]. The GO sample lies on top of an ITO coated quartz slide, which is anchored to a copper plate within an evacuated optical cryostat. Electrical contact is made between the copper plate and a gold pad deposited near the edge of the ITO layer. The sample is illuminated with light from an optical parametric amplifier (OPA) which emits a series of 120 fs light pulses at a 1 kHz repetition rate. The output power is kept constant at 5 mW, and the photon energy is tuned between 0.5 and 4.0 eV. Light absorption occurs in the GO film, producing electron–hole pairs. (The ITO and quartz are both transparent to light within this energy range, while an opening allows light to pass unabsorbed through the copper ground plate.) The copper plate is floating with respect to the ground electrode. This means that photogenerated dipoles produced anywhere between the gold and copper electrodes will be detected as a voltage on the copper plate. (This "floating probe technique" is a standard method to detect photo-induced charge separation [15–17].)

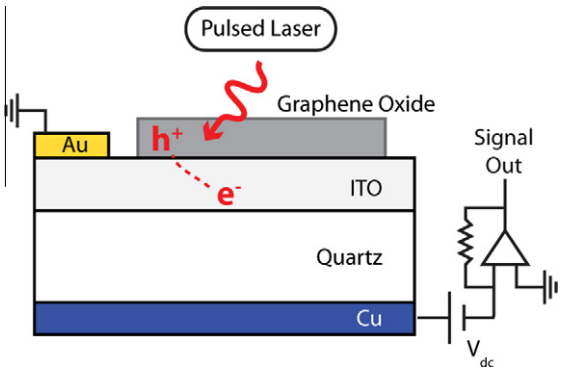

Fig. 1 – Schematic of the capacitive photocurrent spectroscopy measurement set-up.

As observed in organic solar cells, the ITO acts as an acceptor for negative photoexcited charge, causing the electron–hole pairs to separate across the GO/ITO interface. This produces an ac voltage, whose magnitude is proportional to the amount of excited charge, multiplied by the charge separation distance, and whose frequency is equal to the laser repetition rate. An applied DC potential V_{dc} causes the negative charge to be attracted to the ITO/quartz interface, amplifying the capacitive photocurrent signal. The vast majority of the DC bias drops across the quartz, but the small amount of field in the ITO is still sufficient to drive the charge separation. Since the ITO acts as an electron acceptor, a positive voltage must be applied on the Cu plate to attract the negative charge. No signal is observed if the bias is reversed. The voltage is converted to a current through a current amplifier, and detected with a lock-in amplifier synched to the laser repetition rate. Only a small dipole field is necessary to account for the extremely small signal that we measure (currents in the pA range, corresponding to 10^{-8} electrons per photon).

3. Results and discussion

Capacitive photocurrent measurements were performed on three different GO samples. The raw photocurrent data is normalized in units of electrons/photon by dividing the measured photocurrent (in electrons/s) by the number of photons/s (determined by dividing the laser power by the excitation energy). The results are shown in Fig. 2 (blue solid lines). Two of the samples ((a) and (b)) were synthesized in our laboratory, using the procedure described in the experimental section above, while the sample shown in (c) was purchased from a commercial supplier (Graphene Supermarket). Three peaks are observed at approximately 0.7, 1.6 and 3.2 eV and are marked as ▲, ●, and ■). Strong minima occur at 2.1 eV, and beyond 4 eV, indicating gaps in the density of states. Similar results are observed for all three GO samples, although there are variations in the peak position and magnitude. A

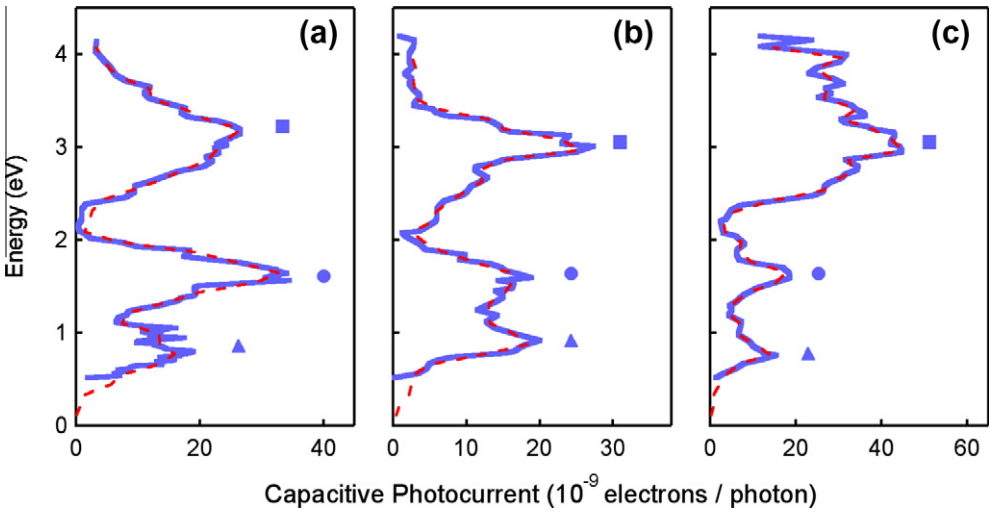

Fig. 2 – Capacitive photocurrent spectra of three GO samples (solid blue line). Three peaks are observed at 0.7, 1.6 and 3.2 eV, (marked as ▲, ●, and ■, respectively). The dashed red curves are calculated following Eq. (2) and using the density of states for GO as shown in Fig. 3. (For interpretation of the references to colour in this figure legend, the reader is referred to the web version of this article.)

comparison to the literature shows that there is a correlation between the two higher energy peaks in the CPS and previous optical spectroscopy measurements of GO. The ●-transition at 1.6 eV is very close to the peak luminescence energy (1.65 eV) emitted from a GO sample in solution [6]. The ■-transition at 3.2 eV (corresponding to a wavelength of 388 nm) is near the shoulder in the absorbance spectrum of GO observed at 320 nm, and also close to the wavelength of blue luminescence observed for partially reduced GO (390 nm) [8]. While the transitions match reasonably well, precise comparisons between our samples and those in the literature are difficult since the reported luminescence peaks are very broad, and variations are observed due to the geometry of the GO sample [7], and the background pH [6]. The observed peaks could also be affected by the environment in contact with the GO, which is known to broaden, or shift the PL spectrum [8].

Since the capacitive photocurrent measures absorption due to the formation of charge carriers, the data can be understood using the standard description for electron band-to-band transitions. The capacitive photocurrent signal $C(h\nu)$ is proportional to the product of the initial and final states integrated over all possible transitions for a given excitation energy $h\nu$, or

$$C(h\nu) = \kappa \int_{E_F - h\nu}^{E_F} D(E)D(E + h\nu)dE \quad (1)$$

where $D(E)$ is the density of states in the GO, E_F is the Fermi energy, and κ is a proportionality constant. To simplify the analysis, we assume that the probability for all different possible transitions is equal (κ held constant), and that all states below the Fermi energy are filled, while states above the Fermi energy are empty (zero temperature approximation) [18,19].

For GO, the DOS is unknown, so it is not possible to calculate $C(h\nu)$ directly from Eq. (1). However, using the capacitive photocurrent spectrum and working backwards from Eq. (1), it is possible to obtain a fit of $D(E)$ to the experimental data. The analysis is as follows (see Supplementary information for a detailed description of the fitting procedure). The capacitive photocurrent C_i is measured for a set of equally spaced excitation energies, $h\nu = i \times \Delta E_i$ where i is an integer ranging from i_{min} to i_{max}, and ΔE is the excitation energy spacing. This leads to the following discretized version of Eq. (1):

$$C_i = \kappa \sum_{j=1}^{i} D_{-j} D_{(i-j)} + 1 \quad (2)$$

Here, $D_{\pm j}$ is defined at energies $E_{+j} = E_F + (j + 1/2)\Delta E$ for empty states above the Fermi energy, and $E_{-j} = E_F - (j - 1/2)\Delta E$ for filled states below the Fermi energy for j ranging from 1 to i_{max}. This gives a set of $(i_{max} - i_{min} + 1)$ coupled equations which together contain $2 \times i_{max}$ different D_j values. In practice, an interpolation is first done from the measured data so that in all cases $\Delta E = 0.11$ eV, $i_{min} = 5$, and $i_{max} = 37$.

Because there are more than twice as many unknown D_j values as there are equations, it is impossible to solve for D_j exactly. Instead, a fitting procedure is used. All values of D_j are initially set to an arbitrary constant. Next, one of the D_j is chosen at random, and the Levenberg–Marquardt algorithm is used to determine the value for this D_j that provides the best possible fit to the experimental measurements (keeping all other D values fixed). This is repeated until a fit has been done for each D_j. The entire process is then repeated until a stable set of D_j values has been obtained. This fitting algorithm is found to generate a reproducible and stable $D(E)$ versus energy dependence, from which a close approximation to the observed capacitive photocurrent spectrum can be obtained.

Fig. 3 shows the GO DOS determined by applying this procedure to the three capacitive photocurrent spectra shown in Fig. 2, while the dashed red lines in Fig. 2 show the capacitive photocurrent calculated from the extracted GO DOS. (The excellent match between the experimental and theoretical

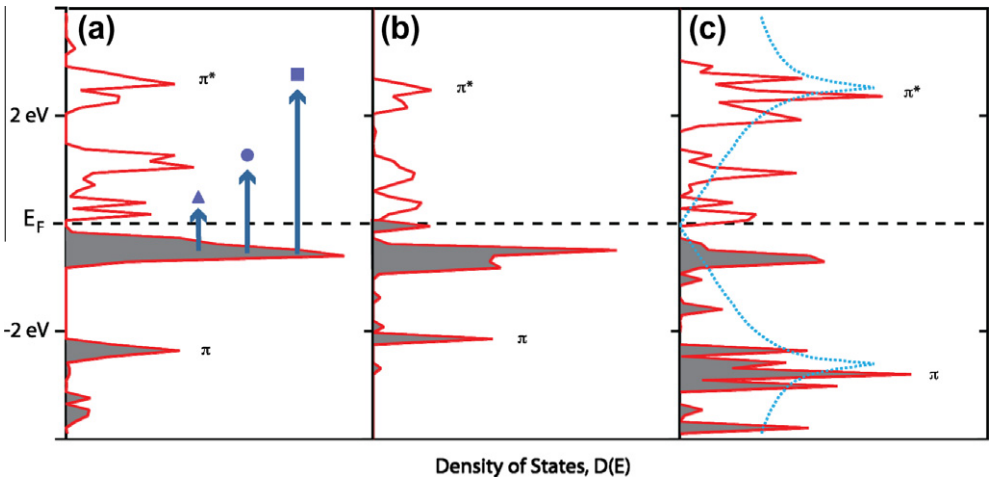

Fig. 3 – Predicted density of states for GO following the fitting of Eq. (2) to the data plotted in Fig. 2. Transitions between the filled and empty states (as shown by the ▲, ●, and ■ transitions in (a)) produce the peaks observed in the capacitive photocurrent. The dashed blue line in (c) is the calculated DOS for graphene. (For interpretation of the references to colour in this figure legend, the reader is referred to the web version of this article.)

capacitive photocurrent spectra demonstrates that the fitting procedure is working properly). There is a clear variation between the DOS calculated for the different samples, but each also contains a similar set of peaks which provide for the transitions observed in the photocurrent. There are two high energy peaks in the GO DOS near ±2.6 eV which are approximately symmetric to the Fermi energy, and three mid-gap features, one occupied below the Fermi energy, and two empty above the Fermi energy. For comparison, the density of states for graphene is also shown, calculated using the tight binding dispersion relation with an overlap integral of 2.6 eV. The high energy peaks at ±2.6 eV correlate reasonably well with the π and π^* peaks expected for the graphene DOS, and are marked as such in the figure. Their presence implies that some influence from the graphene still remains, even in the oxidized sample, and agrees with the picture that there is significant inhomogeneity of the oxidation coverage within the GO plane [4,5,20,21]. Note that the π and π^* peaks are not expected to be precisely symmetric with respect to the Fermi energy because the sample can be doped by the interaction with the substrate or the environment. The amount of this doping varies from sample to sample. Comparison of the capacitive photocurrent data to the calculated density of states shows that the three peaks in the data can be accounted for by transitions from the lowest energy occupied peak to the three lowest energy unoccupied peaks (marked as ▲, ●, and ■ in Fig. 3(a)).

To see the effect of reduction on the GO density of states, capacitive photocurrent measurements were also performed on three different rGO samples. The results are plotted in Fig. 4. As with the GO, two of the samples ((a) and (b)) were synthesized in our laboratory, while the other sample (shown in (c)) was purchased (Graphene Supermarket). The spectra are more complicated, and less similar to each other than with the GO samples. In general, three peaks (marked as ▲, ●, and ■) are once again observed, but they now lie on a gradually increasing background. Applying the described fitting procedure to this data, we extract the DOS plots shown in Fig. 5 (where once again the calculated graphene DOS is included for comparison). The peaks observed in the GO DOS are still visible, however, a number of additional peaks fill the hard gaps where $D(E)$ dropped to zero in the GO. As shown by the dashed line in Fig. 4, the capacitive photocurrent calculated from this density of states provides a good fit to the measured result.

From these results it is clear that the GO reduction does not completely remove the influence of the oxidation and return the sample to a pristine state. It has been demonstrated that GO reduction does not completely quench the luminescence, and thus the recombination centers due to the oxygen must still be present [4,6,8,20,21]. Recently, Gmez-Navarro et al. has shown that rGO consists of fully reduced graphene areas in a matrix of partially reduced graphene oxide with clustered defects [22]. Presence of additional peaks in the DOS of rGO can be attributed to the combination of the DOS due to graphene and the energy states originating due to these clustered defects. Also, the energy of the states due to the oxygen does not change with reduced oxygen coverage. Instead, there is simply a decrease in the average electronic density at the peak energies. This implies that there is considerable inhomogeneity in the oxygen coverage, and that it cannot be assumed that the oxygen occupies the graphene surface in a few stable, well defined uniform configurations [4,5].

To identify the functional groups existing in the GO and rGO samples X-ray photoelectron spectroscopy (XPS) data are presented in Fig. 6. After subtracting a constant background, X-ray photoelectron spectra of the carbon 1s level are de-convoluted into various components using Gaussian peak line shapes. As reported in the literature, the resulting de-convoluted peaks can be attributed to the different functional groups of the carbon atom [20,21]. The GO and rGO samples, all show evidence for the graphitic non-oxygenated C ring (C–C, ~284.6 eV), the C–O single bond (~286.2 eV), the C=O double bond (~287.8 eV) and the O–C=O groups (~289.1 eV) [20]. The peak intensity varies considerably

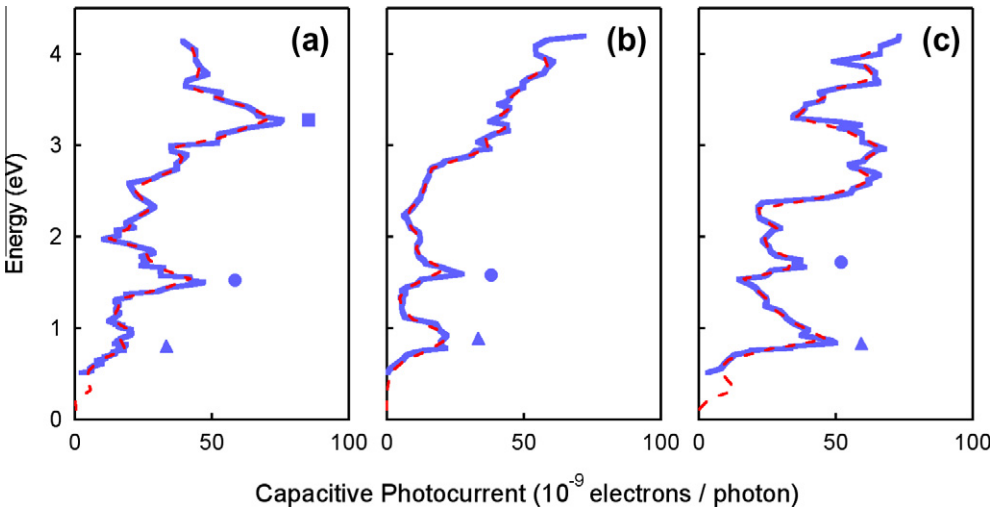

Fig. 4 – Capacitive photocurrent spectra of rGO (solid blue curves). Three peaks, on top of a monotonically increasing background, are observed at 0.7, 1.6 and 3.2 eV, (marked as ▲, ●, and ■, respectively). The dotted curve is calculated following Eq. (1) and using the density of states for rGO as shown in Fig. 5. (For interpretation of the references to colour in this figure legend, the reader is referred to the web version of this article.)

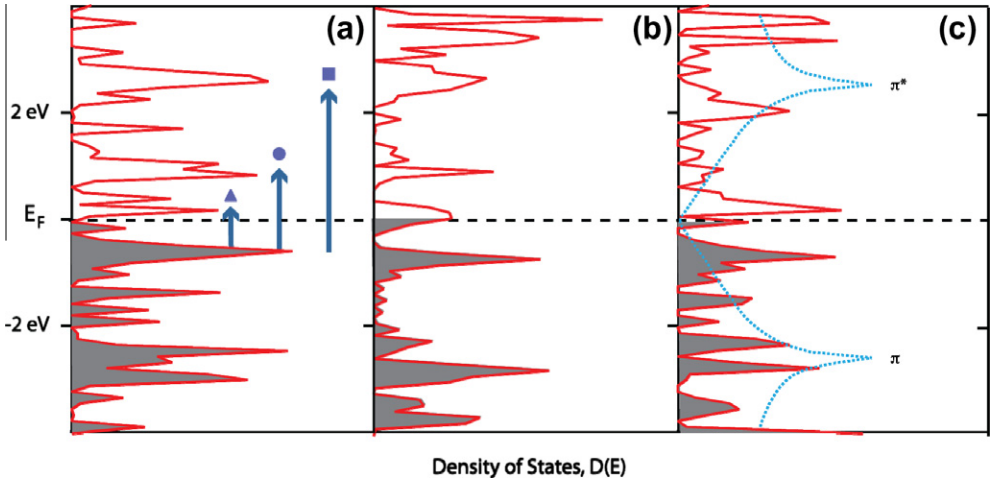

Fig. 5 – Predicted density of states for rGO following the fitting of Eq. (2) to the data plotted in Fig. 4. Transitions between the filled and empty states (as shown by the ▲, ●, and ■ transitions in (a)) produce the peaks observed in the capacitive photocurrent. The dashed blue line in (c) is the calculated DOS for graphene. (For interpretation of the references to colour in this figure legend, the reader is referred to the web version of this article.)

between the different samples, with the peaks associated with the oxygen groups being stronger in the GO sample than in the rGO. In addition, the rGO sample has one extra component at 285.9 eV, indicating the presence of a carbon–nitrogen group. The nitrogen is presumably introduced during the reduction process [20,21].

There is still a great deal of uncertainty concerning the chemical and electronic structure of GO, however, our results generally agree with previously published optical absorbance and luminescence measurements. Our calculated DOS for GO roughly consists of the two π/π^* peaks, plus three additional mid gap states at −0.5, 0.4 and 1.5 eV. Published absorbance measurements of GO clearly show a peak due to the π/π^* transitions of C=C [7,8,23], supporting our assignment of the π/π^* states to the high energy features appearing in our calculated DOS. The available energy range of our laser system is not large enough to observe the direct transition between the π/π^* states, however. The ■ transition in the CPS has an energy of 3.2 eV (corresponding to a wavelength of 388 nm) which correlates reasonably well with the 320 nm shoulder observed in the absorbance spectra of GO. This has been attributed to n–π^* transitions of C=O [8,23]. In our DOS calculation, it is seen as a transition between a mid-gap state at −0.5 eV and the π^* state, suggesting that the −0.5 eV state is the non-bonding orbital of the oxygen atoms [23]. The presence of C=O double bonds are also indicated by the XPS measurements. The ● transition has energy of approximately 1.65 eV (corresponding to wavelength of 750 nm) which is equal to the peak luminescence energy emitted from a GO sample in solution. This peak has been attributed to a

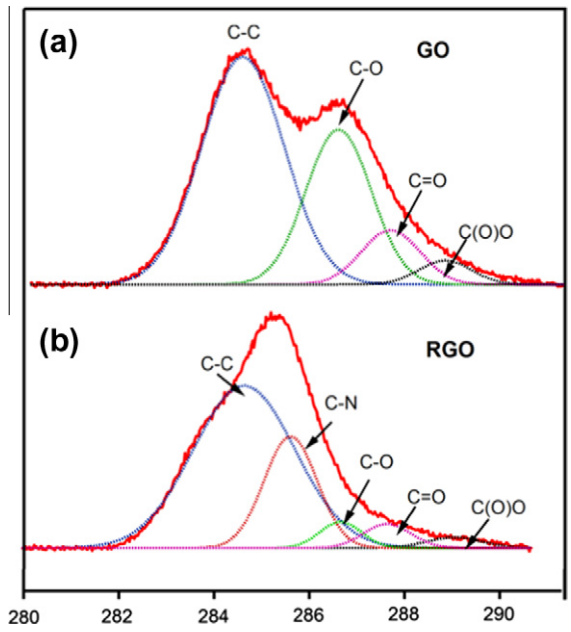

Fig. 6 – X-ray photoelectron spectra (red curves) of (a) GO and (b) rGO samples with de-convoluted components (light colored curves). (For interpretation of the references to colour in this figure legend, the reader is referred to the web version of this article.)

localized energy state at the oxidation sites [24], and from this information, we can tentatively ascribe the 1.5 eV states in the DOS to the carboxyl groups. The ▲ transition at 0.65 eV is an outlier that does not match any feature previously observed in the optical and absorbance spectra of GO. (We note though that previous experiments have not focused on this low energy regime.) Theory suggests that sp^2 clusters isolated within a sp^3 matrix result in energy gaps of around 0.5 eV. However, this would require well organized oxygen coverage on a carbon surface, something that is not indicated by our measurements, or TEM images of the GO surface [25].

4. Conclusion

In summary, we describe a direct experimental probe of the GO density of states for two different oxygen coverages using capacitive photocurrent spectroscopy. Three additional peaks in the DOS of GO appear near the Fermi energy along with standard π/π^* peaks present in graphene DOS. Reduced graphene oxide (rGO) shows three less intense additional peaks with no hard gaps near Fermi energy as seen for the GO sample providing the evidence of some residual oxidation. XPS measurements confirm the presence of similar oxygen functional groups in all the samples (GO and rGO) with varying intensity dictating the oxidation content percentage.

Acknowledgements

We appreciate support from Department of Energy (Grant No. DE-FG02-07ER46375) and National Science Foundation (Grant No. NSF-DMR-0906961).

Appendix A. Supplementary data

Supplementary data associated with this article can be found, in the online version, at doi:10.1016/j.carbon.2011.09.037.

REFERENCES

[1] Novoselov KS, Geim AK, Morozov SV, Jiang D, Zhang Y, Dubonos SV, et al. Electric field effect in atomically thin carbon films. Science 2004;306:666–9.
[2] Wu X, Sprinkle M, Li X, Ming F, Berger C, de Heer, WA. Epitaxial-graphene/graphene-oxide junction: an essential step towards epitaxial graphene electronics. Phys Rev Lett 2008;101:026801.
[3] Gierz I, Riedl C, Starke U, Ast CR, Kern K. Atomic hole doping of graphene. Nano Lett 2008;8:4603–7.
[4] Boukhvalov DW, Katsnelson MIJ. Modeling of graphite oxide. J Am Chem Soc 2008;130:10697–701.
[5] Lahaye RJWE, Jeong HK, Park CY, Lee YH. Density functional theory study of graphite oxide for different oxidation levels. Phys Rev B 2009;79:125435.
[6] Luo Z, Vora PM, Mele EJ, Johnson ATC, Kikkawa JM. Photoluminescence and band gap modulation in graphene oxide. Appl Phys Lett 2009;94:111909.
[7] Sun X, Liu Z, Welsher K, Robinson JT, Goodwin A, Zaric S, et al. Nano-graphene oxide for cellular imaging and drug delivery. Nano Res 2008;1:203–12.
[8] Eda G, Lin Y, Mattevi C, Yamaguchi H, Chen H, Chen I, et al. Blue photoluminescence from chemically derived graphene oxide. Adv Mater 2010;22:505–9.
[9] Mohite AD, Chakraborty S, Gopinath P, Sumanasekera GU, Alphenaar BW. Displacement current detection of photoconduction in carbon nanotubes. Appl Phys Lett 2005;86:061114.
[10] Mohite AD, Santos TS, Moodera JS, Alphenaar BW. Observation of the triplet exciton in EuS-coated single-walled nanotubes. Nat Nanotechnol 2009;4:425–9.
[11] Clark BJ, Frost T, Russell MA. UV spectroscopy techniques, instrumentation, data handling. Chapman and Hall 1993:6–11.
[12] Hummers WS, Offeman RE. Preparation of graphitic oxide. J Am Chem Soc 1958;80:1339.
[13] Kovtyukhova NI, Ollivier PJ, Martin BR, Mallouk TE, Chizhik SA, Buzaneva BV, et al. Layer-by-layer assembly of ultrathin composite films from micron-sized graphite oxide sheets and polycations. Chem Mater 1999;11:771–8.
[14] Gao W, Alemany LB, Ci L, Ajayan PM. New insights into the structure and reduction of graphite oxide. Nat Chem 2009;1:403–8.
[15] Kronik L, Shapira Y. Surface photovoltage phenomena: theory, experiment, and applications. Surf Sci Rep 1999;37:1–206.
[16] Schroder, DK, Semiconductor material and device characterization. John Wiley and Sons 2006: 523–563.
[17] Groves C, Reid OG, Ginger DS. Heterogeneity in polymer solar cells: Local morphology and performance in organic photovoltaics studied with scanning probe microscopy. Acc Chem Res 2010;43(5):612–20.
[18] Bouizem Y, Belfedal A, Sib JD, Chahed L. Density of states in hydrogenated amorphous germanium seen via optical absorption spectra. Solid State Commun 2003;126:675–80.
[19] Bouzerar R, Zeinert A, Von Bardeleben HJ. Correlation of optical absorption and density of paramagnetic centers in a-C:H films. Diamond Relat Mater 2005;14:1108–11.

[20] Stankovich S, Dikin DA, Piner RD, Kohlhaas KA, Kleinhammes A, Jia Y, et al. Synthesis of graphene-based nanosheets via chemical reduction of exfoliated graphite oxide. Carbon 2007;45:1558–65.
[21] Waltman RJ, Pacansky J, Bates CW. X-ray photoelectron spectroscopic studies on organic photoconductors: evaluation of atomic charges on chlorodiane blue and *p*-(Diethylamino)Benzaldehyde Diphenylhydrazone. Chem Mater 1993;5:1799–804.
[22] Gómez-Navarro C, Meyer JC, Sundaram RS, Chuvilin A, Kurasch S, Burghard M, et al. Atomic structure of reduced graphene oxide. Nano Lett 2010;10:1144–8.
[23] Luo Z, Lu Y, Somers LA, Johnson ATC. High yield preparation of macroscopic graphene oxide membranes. J Am Chem Soc 2009;131:898–9.
[24] Gokus T, Nair RR, Bonetti A, Böhmler M, Lombardo A, Novoselov KS, et al. Making graphene luminescent by oxygen plasma treatment. AcsNano 2009;3(12):3963–8.
[25] Erickson K, Erni R, Lee Z, Alem N, Gannett W, Zettl A. Determination of the local chemical structure of graphene oxide and reduced graphene oxide. Adv Mater 2010;22:4467–72.